Finding the Resistance Distance and Eigenvector Centrality from the Network's Eigenvalues

Caracé Gutiérrez,[1] Juan Gancio,[1] Cecilia Cabeza,[1] and Nicolás Rubido[2,1,*]

[1] *Universidad de la República, Instituto de Física de Facultad de Ciencias, Iguá 4225, Montevideo 11400, Uruguay.*
[2] *University of Aberdeen, Aberdeen Biomedical Imaging Centre, AB25 2ZG Aberdeen, United Kingdom.*

(Dated: January 15, 2021)

There are different measures to classify a network's data set that, depending on the problem, have different success rates. For example, the resistance distance and eigenvector centrality measures have been successful in revealing ecological pathways and differentiating between biomedical images of patients with Alzheimer's disease, respectively. The resistance distance measures an effective distance between two nodes of a network taking into account all possible shortest paths between them and the eigenvector centrality measures the relative importance of each node in a network. However, both measures require knowing the network's eigenvalues and eigenvectors. Here, we show that we can closely approximate [find exactly] the resistance distance [eigenvector centrality] of a network only using its eigenvalue spectra, where we illustrate this by experimenting on resistor circuits, real neural networks (weighted and unweighted), and paradigmatic network models – scale-free, random, and small-world networks. Our results are supported by analytical derivations, which are based on the eigenvector-eigenvalue identity. Since the identity is unrestricted to the resistance distance or eigenvector centrality measures, it can be applied to most problems requiring the calculation of eigenvectors.

PACS numbers: 02.10.Ox, 89.75.-k, 89.75.Fb, 89.75.Hc
Keywords: Resistor Networks, Resistance Distance, Eigenvector Centrality, Eigenvalue spectra

I. INTRODUCTION

From human brain studies to social network analyses, we have seen enormous improvements in terms of data availability and accuracy. High-resolution brain scans are allowing us to study the brain's functional connectivity with increasing detail [1–3], which in turn, helps us to understand cognitive processes or the effects that diseases cause to the brain's connectivity. Social network platforms, such as Twitter and Facebook, produce unprecedented data streams, which, for example, allows us to study how information is shared among different communities [4, 5]. However, with an increasing ability to obtain larger and more reliable data sets, we also need to improve our data mining abilities. In this mining process, network analysis has proven useful [6].

Network science provides us with different measures to characterise, classify, and extract information from network data sets [7, 8]. Namely, measurable quantities that highlight the most relevant relationships appearing within the elements of the data set. In general, relevant measures are typically the invariant ones [9], i.e., those that when nodes (elements in the data set) are relabelled, the measure remains unchanged. In particular, the eigenvalue spectra and eigenvector set are such measures. Moreover, these spectral characteristics have been shown to relate with other topological measures, such as the degree distributions [10–12], centrality measures [13–15], and modularity [16–18].

An important measure to quantify distance between nodes in a network is the resistance distance [21–24], which is found from the network's eigenvalues and eigenvectors. This measure includes more information than the shortest-path joining two nodes, which is defined by the minimum number of edges (links) necessary to connect the nodes in a series path. The resistance distance also takes into account all other (non-repeating) paths connecting the two nodes to add them as parallel paths [21, 24–27]. Hence, shortest-paths are relevant when there is a known corpuscular communication along the edges of the network, whilst the resistance distance is relevant when communication along the edges is spread like a wave pattern (as it happens in several extended systems). For example, the resistance distance has been used to detect communities (i.e., group nodes into modules) [28–30], explain transport phenomena [31–34], analyse the global robustness of a network [35, 36], describe stochastic growth processes [37–39], and reveal gene flows [40] or ecological pathways [41, 42].

Another relevant measure is the eigenvector centrality, which quantifies the relative importance of each node in a network and is based on the network's Perron-Frobenius eigenvector [43]. This measure provides a score to each node according to the positive entries of the eigenvector associated to the largest eigenvalue of the adjacency matrix [15, 44–46]. The eigenvector centrality has been particularly useful in biomedical image analysis [47, 48] for a broad range of studies, such as, Alzheimer's disease [49, 50], type-I diabetes [51], and ageing [52]. Also, it has been used for community detection [53], characterise protein pathways [54], and measure the elastic modulus of materials [55]. Nevertheless, as with the resistance

* nicolas.rubidoobrer@abdn.ac.uk; nrubido@fisica.edu.uy

distance, the eigenvector centrality depends on finding eigenvectors, which for large networks can be computationally demanding. For example, in a QR decomposition, finding all eigenvalues of a size $N \times N$ matrix has a computational cost of $\mathcal{O}(N^2)$, whilst finding its eigenvectors costs $\mathcal{O}(N^3)$ [56]. Basically, the reason behind this is that eigenvectors are found from solving N linear algebraic equations, whilst eigenvalues are found from solving an N-degree polynomial.

Here we show that, we can closely approximate the resistance distance and exactly find the eigenvector centrality of weighted or unweighted networks with their eigenvalue spectra. Our method is based on the recent works by Denton et al. [19, 20], who recently recovered an algebraic relationship to find the magnitudes of eigenvector's components from their eigenvalue spectra. Our results include analytical expressions that we apply in small-sized resistor circuits ($N \sim \mathcal{O}(10^1)$), cortical connectivity networks [57] ($N \sim \mathcal{O}(10^2)$), and synthetically generated network-models ($N \sim \mathcal{O}(10^3)$). Specifically, we generate scale-free [58], random [59], and small-world networks [60]. We note that, aside cases where the network has a degenerate eigenvalue spectra, our conclusions are general and unrestricted to these topological measures and examples.

II. METHODS

Denton et al. [19, 20] have recently shown that the components of eigenvectors can be recovered from the eigenvalue spectra, which they name as *eigenvector-eigenvalue identity*, and is valid for any Hermitian matrix (i.e., a matrix A whose identical to its conjugate transpose) with non-degenerate eigenvalues (i.e., repeated eigenvalues, which span an eigenspace with more than 1 eigenvector). This identity has been discovered and rediscovered in linear algebra for almost two centuries, with Jacobi (1834) being one of the earliest references [61]. Specifically,

$$\left|[\vec{\psi}_n]_i\right|^2 = \frac{\prod_{k=1}^{N-1}\left[\lambda_n(\mathbf{A}) - \lambda_k(\mathbf{M}_i)\right]}{\prod_{k=1;\, k\neq n}^{N}\left[\lambda_n(\mathbf{A}) - \lambda_k(\mathbf{A})\right]}, \qquad (1)$$

where $[\vec{\psi}_n]_i$ is the i-th component ($i = 1, \ldots, N$) of the n-th eigenvector of matrix $\mathbf{A}$ associated to the eigenvalue $\lambda_n(\mathbf{A})$ (with $n = 1, \ldots, N$ modes), such that $\mathbf{A}\vec{\psi}_n = \lambda_n(\mathbf{A})\vec{\psi}_n$, and $\lambda_k(\mathbf{M}_i)$ is the k-th eigenvalue ($k = 1, \ldots, N-1$) of matrix $\mathbf{M}_i$, which is obtained from $\mathbf{A}$ by removing the i-th row and column. Also, without loss of generality, it can be assumed that the eigenvalue spectra in Eq. (1) is ordered non-decreasingly; that is, $\lambda_1(\mathbf{A}) \leq \lambda_2(\mathbf{A}) \leq \cdots \leq \lambda_N(\mathbf{A})$. Consequently, Eq. (1) allows to find the magnitudes for all the eigenvector components of matrix $\mathbf{A}$ from its eigenvalues.

In this work, matrix $\mathbf{A}$ is the network's adjacency matrix. We restrict ourselves to analyse undirected networks, which correspond to having Hermitian adjacency matrices, i.e., symmetric and with non-negative entries. Namely, $A(i,j) = A(j,i) \geq 0$ for all entries ($\mathbf{A} = \mathbf{A}^T$), where $A(i,j) > 0$ if node i is connected to node j, and $A(i,j) = 0$ otherwise. In particular, we construct small-sized resistor networks in almost ring-like structures with $N = 6$, 12, 18, and 24 nodes [25, 26]. These adjacency matrices are such that, $A(i,j) = (1.00 \pm 0.01)\, k\Omega$ [Ohm] (1% accurate according to the manufacturer) if $j = i \pm 1$ (modulus N) and 0 otherwise, with an extra edge (resistor) connecting nodes 1 and 3 which break the ring symmetry, i.e., $A(1,3) = (1.00 \pm 0.01)\, k\Omega = A(3,1)$. We add this edge in order to lift the degenerate eigenvalues that are always present in circulant networks [9, 23]. Also, we consider cortical networks from the Brain Connectivity Toolbox [57] data-set, which contain weighted (symmetry is imposed by $\mathbf{A} = (\mathbf{A} + \mathbf{A}^T)/2$) and unweighted adjacency matrices. Also, we generate different random networks for our analysis, using the Barabási-Albert model [58] for scale-free networks, the Erdös-Rényi model [59] for homogeneously random networks, and the Watts-Strogatz model [60] for small-world networks [62].

In order to find the main network-characteristics, such as the average shortest-path and clustering coefficient, we use the Brain Connectivity Toolbox [57]. We find the resistance distance between nodes i and j, $\rho(i,j)$, by using the eigenvalues and eigenvectors of the network's Laplacian matrix, $\mathbf{L} = \mathbf{D} - \mathbf{A}$, where $\mathbf{D}$ is a diagonal matrix containing all the node degrees (i.e., the number of neighbours) and $\mathbf{A}$ is the network's adjacency matrix. Specifically, $\rho_{theo}(i,j)$ can be found from [21–24]

$$\rho_{theo}(i,j) = \sum_{n=2}^{N} \frac{1}{\lambda_n(\mathbf{L})} \left|[\vec{\phi}_n]_i - [\vec{\phi}_n]_j\right|^2, \qquad (2)$$

where $\mathbf{L}\vec{\phi}_n = \lambda_n(\mathbf{L})\vec{\phi}_n$ for $n = 1, \ldots, N$. It is worth noting that when $\mathbf{A} = \mathbf{A}^T$ the Laplacian matrix is positive semi-defined [9], implying that the eigenvalues, $\lambda_n(\mathbf{L})$, are always such that $0 = \lambda_1(\mathbf{L}) \leq \lambda_2(\mathbf{L}) \leq \cdots \leq \lambda_N(\mathbf{L})$. The resultant $\rho_{theo}(i,j)$ is identical to the one that can be found by applying Kirchhoff's circuit laws, considering all serial and parallel paths between nodes i and j.

III. RESULTS

Here, we derive an approximate value for the resistance distance by finding upper and lower bounds from Eq. (1). We show that our approximation for the resistance distance closely matches the theoretical value [Eq. (2)] in different real-world and synthetic networks. Then, we use Eq. (1) to exactly find the eigenvector centrality measure, which implies that any difference in the numerical calculations appearing in practical applications are due to numerical errors (such as round-off and truncation errors) and can be neglected.

The *resistance distance*, ρ_{theo}, requires knowing the eigenvalue spectra and all eigenvector components' magnitudes and signs. Since the eigenvalue-eigenvector identity of Eq. (1) only allows for the calculation of magni-

tudes, we are unable to know exactly how the differences in Eq. (2) are contributing to the overall $\rho_{theo}(i,j)$ value. However, we can use the eigenvector magnitudes from Eq. (1) to find upper and lower bounds. Specifically, we use Eq. (1) to write the i-th component of $\vec{\psi}_n$ as

$$\left|[\vec{\phi}_n]_i\right|^2 = \frac{\prod_{k=1}^{N-1}\left[\lambda_n(\mathbf{L}) - \lambda_k(\mathbf{M}_i)\right]}{\prod_{k=1;\,k\neq n}^{N}\left[\lambda_n(\mathbf{L}) - \lambda_k(\mathbf{L})\right]}, \qquad (3)$$

where matrix $\mathbf{M}_i$ is now obtained from the network's Laplacian matrix, $\mathbf{L}$, by removing its i-th row and column. On the other hand, the difference between the i-th and j-th coordinates for the n-th mode in Eq. (2) is

$$\left|[\vec{\phi}_n]_i - [\vec{\phi}_n]_j\right|^2 = \left|[\vec{\phi}_n]_i\right|^2 + \left|[\vec{\phi}_n]_j\right|^2 - 2[\vec{\phi}_n]_i[\vec{\phi}_n]_j^*, \quad (4)$$

where the last cross-product term has an unknown sign – it can be either positive or negative, depending on the components' sign of each eigenvector.

We use Eq. (3) to approximate ρ_{theo} as follows. We do the summation in Eq. (2) as if it contain only positive or negative cross-products terms, i.e., either we use $+2|[\vec{\phi}_n]_i||[\vec{\phi}_n]_j|$ or use $-2|[\vec{\phi}_n]_i||[\vec{\phi}_n]_j|$. When only adding [subtracting] these cross-product terms, we are effectively generating an upper [a lower] bound for the resistance distance, which we note as $\rho_{up}(i,j)$ [$\rho_{down}(i,j)$]. We propose to use these bounds to approximate the exact $\rho(i,j)_{theo}$ value by their average, namely,

$$\rho_{approx}(i,j) = \frac{1}{2}\left[\rho_{up}(i,j) + \rho_{down}(i,j)\right], \ \forall\, i,j, \qquad (5)$$

which effectively cancels the cross-product terms,

$$\rho_{approx}(i,j) = \sum_{n=2}^{N} \frac{\left(\left|[\vec{\phi}_n]_i\right|^2 + \left|[\vec{\phi}_n]_j\right|^2\right)}{\lambda_n(\mathbf{L})}, \ \forall\, i,j. \qquad (6)$$

In order to quantify how closely ρ_{approx} is to the exact resistance distance value, ρ_{theo} [Eq. (2)], we find the *average relative error*,

$$\Delta\rho(N) = \frac{2}{N(N-1)}\sum_{i=1}^{N}\sum_{j>i}^{N}\left|1 - \frac{\rho_{approx}(i,j)}{\rho_{theo}(i,j)}\right|. \qquad (7)$$

A. Approximate resistance distance for circuits and cortical networks

As an experimental illustration of how Eq. (6) works, we design resistor circuits for quasi-ring structures (details in Sect. II), measure their equivalent resistance, ρ_{equiv}, and compare them with theoretical resistance-distance values [Eq. (2)] and with our approximation [Eq. (6)]. Results can be seen on Fig. 1. We use an ohmmeter to measure ρ_{equiv} for all pairs of nodes in the

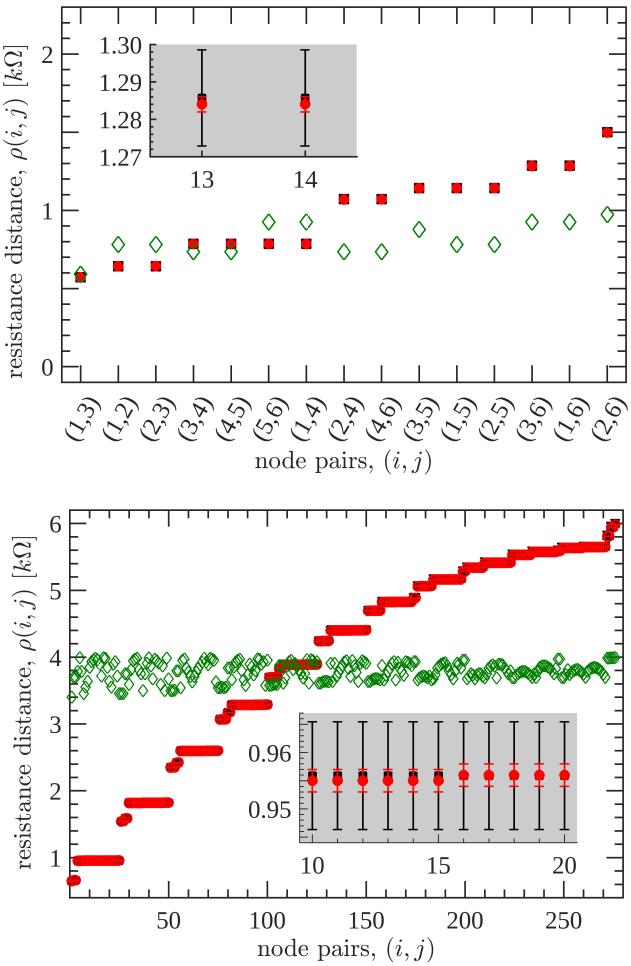

FIG. 1. **Resistance distance values for quasi-ring resistor networks**. Top [Bottom] panel shows the results for $N = 6$ [$N = 24$] nodes, where edges are resistors connected in a ring structure with an extra resistor between nodes 1 and 3. Filled (red online) circles show the ohmmeter readings, filled black squares show the theoretical resistance distance values, ρ_{theo} [Eq. (2)] (assuming identical 1 $k\Omega$ resistors), and unfilled (green online) diamonds show our approximate resistance distance [Eq. (6)]. Edges are ordered according to increasing ρ_{theo} values and are unlabelled in the bottom panel.

circuits, where the ohmmeter's resolution is set to $\approx 1\,\Omega$ [Ohm] ($\approx 0.1\%$). Also, we define synthetic circuits for the theoretical calculations assuming identical 1 $k\Omega$ resistors with a 1% uncertainty for all edges (similar to the 1% uncertainty given by the manufacturer), where we compute the uncertainty in $\rho_{theo}(i,j)$ by error propagation (resulting in a 1% uncertainty for all $\rho_{theo}(i,j)$ values). These experimental and theoretical measures should be same [29], which we corroborate by finding negligible relative-difference between them; $\Delta\rho = 1\times10^{-4}$ for $N = 6$ and 2×10^{-6} for $N = 24$. These negligible differences can be appreciated in the insets of Fig. 1.

As our experimental resistor circuits have a nearly pristine regular-structure (i.e., a ring network with an ex-

tra edge), the approximation fails to follow the exact resistance-distance values, ρ_{theo}. The reason being that pristine networks have degenerate eigenvalues, making Eq. 1 invalid. Both panels of Fig. 1 show that intermediate values of ρ_{theo} – measured from an ohmmeter (filled circles) or calculated from Eq. (2) (filled squares) – are closely approximated by ρ_{approx} (unfilled diamonds), but their extreme values are not (i.e., either for small $\rho(i,j)$ or for large $\rho(i,j)$). In particular, we find that $\Delta\rho \approx 0.25$ for $N = 6$ (top panel) and ≈ 0.5 for $N = 24$ (bottom panel). As we show in what follows, the average relative error, $\Delta\rho$, decreases significantly for complex networks, such as real neural networks (see Fig. 2) and synthetically generated models (see Figs. 4 and 5), where we show that ρ_{approx} follows closely ρ_{theo}.

Figure 2 shows the results for 3 cortical networks taken from the BCT [57] data-set: the Cat's cortical and thalamic areas (top panel), the Macaque's large-scale visual sensorimotor areas (middle panel), and the Macaque's cortical connectivity. We can see in each panel how the approximate ρ_{approx} (unfilled diamonds) follows closely the ρ_{theo} values (filled circles), which are ordered according to the ρ_{theo} magnitudes. More importantly, we note that the Cat's network is weighted (top panel), showing that the approximation also holds for weighted networks. We find that $\Delta\rho = 3.01\%$ for the top panel, 5.68% for the middle panel, and 5.92% for the bottom panel, showing that ρ_{approx} can effectively approximate the exact ρ_{theo} value in complex cortical networks.

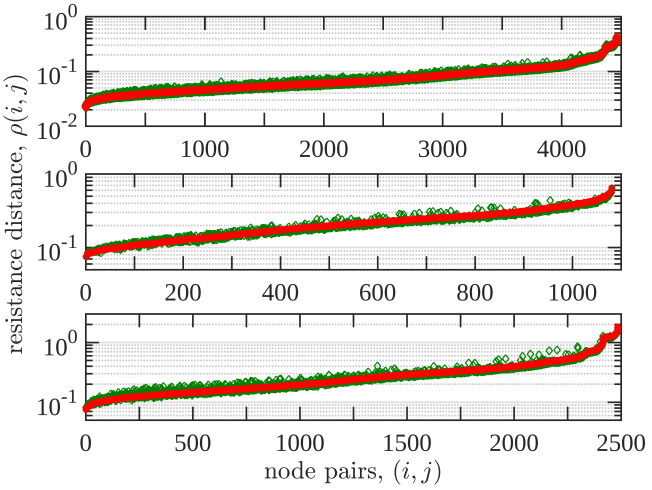

FIG. 2. **Resistance distance for symmetrical cortical networks**. From top to bottom, the panels show the exact, ρ_{theo} (filled circles), and approximate (unfilled diamonds) resistance distance values between all $N\,N(N-1)/2$ pairs of nodes of the Cat's cortical and thalamic areas ($N = 95$ nodes and 1085 weighted links), the Macaque's large-scale visual and sensorimotor areas ($N = 47$ nodes and 313 unweighted links), and the Macaque's cortical connectivity ($N = 71$ nodes and 438 unweighted links) [57]. Edges are ordered according to increasing ρ_{theo} values.

B. Approximate resistance distance for synthetic networks

In order to quantify the effectiveness of the resistance distance approximation, ρ_{approx}, in larger networks, we do the same analysis to scale-free Barabasi-Albert (BA) networks [58], random Erdös-Renyi (ER) networks [59], and small-world Watts-Strogatz (WS) networks [60].

The results for a BA network realisation with 1000 nodes and exponent, $\alpha \simeq 2.5$, where $P(k) \propto k^{-\alpha}$ is the degree distribution, are shown in Fig. 3. We can see that ρ_{approx} (unfilled diamonds) follows closely the ordered values of the exact resistance distance, ρ_{theo} (filled circles) – as in the cortical networks of Fig. 2. We note that we get nearly identical curves (not shown here) for 20 realisations of BA networks with the same topological characteristics (i.e., N and α). For these BA networks, we find that the average relative difference is $\Delta\rho \simeq 0.5\%$, showing a remarkable agreement between the approximate and exact values. The few exceptions appearing in Fig. 3, seem to be almost irrelevant; the reason being the large number of node pairs, which is 3 orders of magnitude larger than the cortical networks. Moreover, using other exponents for BA networks (not shown here), i.e., $2.2 \leq \alpha \leq 3.1$, we find similar results, where the approximated resistance distance follows the exact value for all node pairs in the networks. Overall, the scale-free characteristics of the degree distribution appear to improve the success rate of our approximation in all BA networks.

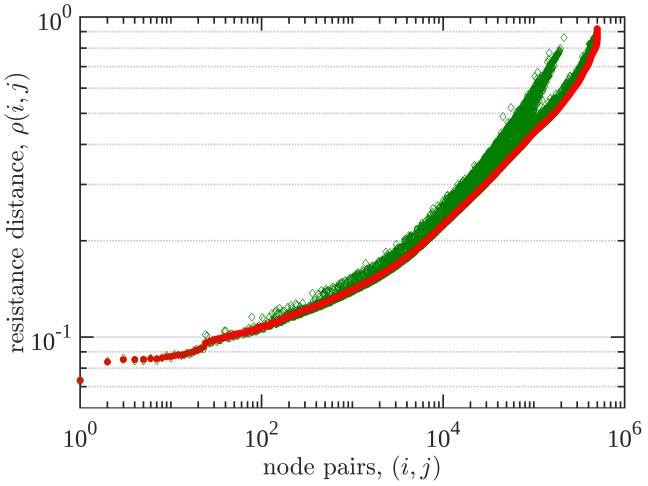

FIG. 3. **Resistance distance for an scale-free network of $N = 1000$ nodes**. The exact and approximate resistance distance values are signalled as in Fig. 2. The degree distribution of this network has a power-law with exponent 2.5.

For the ensemble of ER and WS networks, we compute the normalised average shortest-path, $\langle L\rangle(p)/\max\{\langle L\rangle(p)\}$, average clustering coefficient, $\langle C\rangle(p)/\max\{\langle C\rangle(p)\}$, and resistance distance relative error, $\Delta\rho(p)$, as a function of the attachment or rewiring probability, p, for random networks or small-world net-

works, respectively. The resultant measures are shown in Figs. 4 and 5 by the filled blue (online) squares, black triangles, and red (online) circles, respectively. The normalised average shortest-paths and average clustering coefficient are shown to identify the rewiring probability region where small-world properties emerge [60]; namely, large average-clustering with small average shortest-paths. This region can be seen in Fig. 5, where the small-world characteristics emerge for $10^{-3} \lesssim p \lesssim 10^{-1}$.

We note from Fig. 4 that random networks of $N = 500$ (left panel) and 1000 (right panel) nodes have particularly small resistance distance relative errors, $\Delta\rho \leq 1\% \,\forall\, p$, for all attachment probabilities, p. In particular, we observe that as the random network gets more connected, starting from a giant component at $p_c = \ln(N)/N$ and up to the complete graph at $p = 1$, the average shortest-path (blue squares) decreases steadily, non-trivially (it forms a broken monotonically decreasing curve), but only slightly (1 order of magnitude less than $\langle L(p_c)\rangle$), and that the average clustering coefficient (black triangles) increases as a power-law (increasing 2 orders of magnitude from $\langle C(p_c)\rangle$). More importantly, as the random network gets more connected, the distance between ρ_{approx} and ρ_{theo} [Eq. (2)] decreases (in average) steadily below 1%. Overall, we can conclude that random networks have a resistance distance measure that is excellently approximated by Eq. (6).

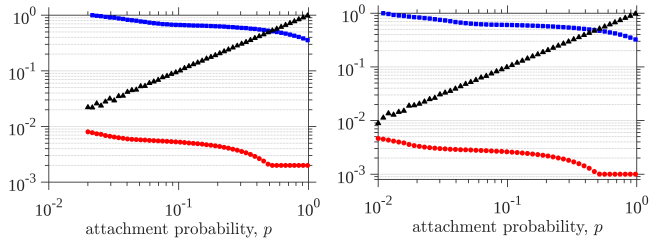

FIG. 4. **Erdös-Rényi network properties as a function of the attachment probability,** p. Panels show the normalised average shortest-path, $\frac{\langle L\rangle(p)}{\langle L\rangle(p_c)}$, average clustering coefficient, $\frac{\langle C\rangle(p)}{\langle C\rangle(1)}$, and resistance distance relative error, $\Delta\rho$, in blue (online) squares, black triangles, and red (online) circles, respectively. These random networks [59] are defined by the attachment probability, p (starting at $p \gtrsim p_c = \ln(N)/N$), and the number of nodes, N, where $N = 5\times10^2$ and $N = 10^3$ for the left and right panels, respectively. These panels are constructed from the average over 10 realisations per p.

On the other hand, from Fig. 5 we observe that small-world networks of $N = 500$ (left panel) and 1000 (right panel) nodes – with initial regular node degree $k = 10$ [60] – have an overall higher $\Delta\rho$ than the random networks. We particularly note this difference in the small-world region, where $\Delta\rho$ only decreases below 10% after the rewiring probability, p, is higher than the one needed for having small-world characteristics. This ending behaviour can be expected, since for $p = 1$ the Watts-Strogatz model is similar to an ER random network. The main difference between random networks and small-world networks is the degree regularity. This stems from the initial network, having a uniform node degree of $K = 10$ at $p = 0$, which is maintained for small rewiring probabilities, $p \lesssim 10^{-2}$. In particular, we can see that $\Delta\rho(p)$ tends to 50% for $p \simeq 10^{-3}$, as in the resistor networks of Fig. 1, which are also nearly regular graphs. Meaning that, networks with small-world characteristics that are closer to regularity than to randomness hinder the success rate of our approximation.

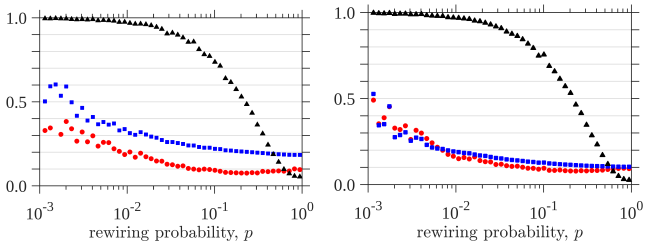

FIG. 5. **Watts-Strogatz network properties as a function of the rewiring probability,** p. Panels show the same metrics and symbols as in Fig. 4. These networks [60] are constructed by an initial regular network with node degree, $K = 10$, and then rewired with probability, p; where the number of nodes, N, is 5×10^2 and 10^3 for the left and right panels, respectively. Small-world characteristics can be identified in the range $10^{-3} < p \lesssim 10^{-1}$.

C. Resistance Distance discussion

Our results show that our approximation for the resistance distance between any two nodes in a network improves with degree-heterogeneity and network size. A heuristic reason for this improvement can be found from analysing the properties of the cross-term from Eq. (2), which is removed in Eq. (6) to obtain our approximate resistance-distance. Namely, we state that

$$\text{cross term} = \sum_{n=2}^{N} \frac{[\vec{\phi}_n]_i [\vec{\phi}_n]_j^*}{\lambda_n(\mathbf{L})} \xrightarrow{N\to\infty} 0. \tag{8}$$

This term is an inner product between the Laplacian spanning eigenvectors (i.e., for $n > 1$) i-th and j-th coordinates, normalised by the corresponding eigenvalue. That is, the inner product between the vectors $\{[\vec{\phi}_2]_i/\lambda_2, \ldots, [\vec{\phi}_N]_i/\lambda_N\}$ and $\{[\vec{\phi}_2]_j/\lambda_2, \ldots, [\vec{\phi}_N]_j/\lambda_N\}$. We also note that the spanning eigenvectors have zero-mean due to orthonormality and fulfil the completeness property [34]; as we show in what follows. Hence, the product between 2 coordinates of any given mode n is likely to change sign for different modes and also add to 0 when all modes are taken into account (completeness). Consequently, these reasons make the sum in Eq. (8) to become approximately null.

For a connected network, the Laplacian eigenvectors are orthonormal, i.e., $\vec{\phi}_n \cdot \vec{\phi}_m = \delta_{nm}$, where $\delta_{nn} = 1$ for

any n and $\delta_{nm} = 0$ for $n \neq m$. In particular, we know that $\vec{\phi}_1 = \vec{1}/\sqrt{N}$, which is the eigenvector associated to the null eigenvalue spanning the kernel. Hence, for $n > 1$, $0 = \vec{\phi}_n \cdot \vec{\phi}_1 = \sum_{i=1}^{N} [\vec{\phi}_n]_i/\sqrt{N}\ \forall\, n > 1$, which means that all $\vec{\phi}_{n>1}$ have zero mean. This means that the coordinates of any spanning eigenvector must have different signs. We also note that by completeness,

$$\sum_{n=1}^{N} [\vec{\phi}_n]_i [\vec{\phi}_n]_j^* = \delta_{ij}, \tag{9}$$

which means that $\sum_{n=2}^{N} [\vec{\phi}_n]_i [\vec{\phi}_n]_j^* = \delta_{ij} - 1/N$. Overall, Eq. (8) then is a variation of this completeness equation, that due to the eigenvalue modulations – $1/\lambda_n$ in Eq. (8)) – and large N, tends to be close to zero.

D. Obtaining the eigenvector centrality from eigenvalues

We now briefly show how to find the network's *eigenvector centrality*, $\vec{\psi}^{(c)} = \vec{\psi}_N = \{\psi_1^{(c)}, \ldots, \psi_N^{(c)}\}$, from Eq. (1). $\vec{\psi}^{(c)}$ is the Perron-Frobenius eigenvector associated to the maximum eigenvalue [43] of the adjacency matrix, $\max_{n=1,\ldots,N}\{\lambda_n(\mathbf{A})\} = \lambda^{(c)}$. This means that $\vec{\psi}^{(c)}$'s components are non-negative, i.e., $\mathbf{A}\vec{\psi}^{(c)} = \lambda^{(c)}\vec{\psi}^{(c)}$ with $[\vec{\psi}^{(c)}]_i = \psi_i^{(c)} \geq 0\ \forall\, i$, and they represent the relative importance that each node has in the network. More importantly, this means that Eq. (1) can be used directly to find its components by

$$\left|[\vec{\psi}^{(c)}]_i\right|^2 = \left|[\vec{\psi}_N]_i\right|^2 = \frac{\prod_{k=1}^{N-1}\left[\lambda_N(\mathbf{A}) - \lambda_k(\mathbf{M}_i)\right]}{\prod_{k=1}^{N-1}\left[\lambda_N(\mathbf{A}) - \lambda_k(\mathbf{A})\right]}, \tag{10}$$

where we assume (without loss of generality) that the eigenvalue spectra ordering is non-decreasing; that is, $\lambda_1(\mathbf{A}) \leq \lambda_2(\mathbf{A}) \leq \cdots \leq \lambda_N(\mathbf{A})$. Consequently, Eq. (10) gives the exact eigenvector centrality measure for any Hermitian adjacency matrix (i.e., for any weighted or unweighted networks) only using its eigenvalue spectra.

IV. CONCLUSIONS

In this work, we use the eigenvector-eigenvalue identity to express network measures that are based on eigenvectors and/or eigenvalues, only in terms of the eigenvalues. Although our works focuses on the resistance distance and on how to use the identity to obtain the eigenvector centrality, it is unrestricted to these measures and can be directly extended to any topological measure that requires knowing eigenvector sets. The only limit to our approach is having a connected network without degenerate eigenvalues (or closely degenerate eigenvalues). This implies that we cannot obtain approximations for the resistance distance (or the exact central eigenvector) for directed networks, where eigenvalues become complex numbers, or regular networks, such as crystalline structures, where degenerate eigenvalues are present.

On the one hand, we derive an expression to approximate the resistance distance, ρ_{approx} [Eq. (6)], values of a network from its Laplacian matrix eigenvalue spectra. We first use experimentally implemented, small-sized, resistor networks to explain how our approximation works [see Fig. 1]. We then show how efficiently our approximation matches the exact resistance distance values. Specifically, we test it on real-world connectivity networks [Fig. 2] and on synthetically generated scale-free [Fig. 3], random [Fig. 4], and small-world networks [Fig. 5]. From these numerical experiments, we conclude that ρ_{approx} in scale-free and random networks typically misses the exact value by less than 1%, regardless of the attachment probability [see Figs. 3 and 4]. More importantly, we can successfully approximate the resistance distance of the cortical networks analysed, with smaller relative differences than 5%. For small-world networks, the approximation misses by 50% when the network is almost regular ($p \simeq 0$), decreasing its relative error steadily from 50% to 10% during the small-world region as edges are rewired [see Fig. 5]. These ineffective approximations are due to the inherent regularity of small-world networks, which have an initial regular structure that contains degenerate eigenvalues, making the eigenvector-eigenvalue identity a false approximation for the eigenvector magnitudes. Consequently, we expect that our ρ_{approx} will always work better for networks that have an heterogeneous (and broad) degree distribution – such as those from real-world complex systems – than for those with a narrow degree distribution.

On the other hand, we show that the eigenvector centrality of a network can have an expression that only depends on the eigenvalues of its adjacency matrix. When eigenvalues are non-degenerate, our expression allows to find the eigenvector centrality measure without the need to find the adjacency matrix eigenvectors, which is computationally demanding for large-sized networks. Consequently, and given the current relevance that the eigenvector centrality measure is having in current biomedical research, such as in [47–52] (e.g., in Network Neuroscience), we believe our expression will become increasingly useful as larger cortical networks are analysed.

ACKNOWLEDGMENTS

C.G. acknowledges funds from the Agencia Nacional de Investigación e Innovación (ANII), Uruguay, POS_NAC_2018_1_151237. J.G. acknowledges funds from the ANII, Uruguay, POS_NAC_2018_1_151185. All authors acknowledge the Comisión Sectorial de Investigación Científica (CSIC), Uruguay, group grant "CSIC2018 - FID13 - grupo ID 722".

[1] Bullmore, E., & Sporns, O. (2009). Complex brain networks: graph theoretical analysis of structural and functional systems. *Nature Rev. Neurosci.*, **10**(3), 186-198.

[2] Papo, D., Zanin, M., & Buldú, M. J. (2014). Reconstructing functional brain networks: have we got the basics right?, *Frontiers in Human Neurosci.*, **8** (2014) 107.

[3] Fornito, A., Zalesky, A., & Bullmore, E. *Fundamentals of brain network analysis* (Academic Press, 2016).

[4] Wasserman, S., & Faust, K. *Social network analysis: Methods and applications* (Vol. 8. Cambridge university press, 1994).

[5] Pastor-Satorras, R., Rubi, M., & Diaz-Guilera, A. (Eds.). *Statistical mechanics of complex networks* (Vol. 625. Springer Science & Business Media, 2003).

[6] Zanin, M., Papo, D., Sousa, P. A., Menasalvas, E., Nicchi, A., Kubik, E., & Boccaletti, S. (2016). Combining complex networks and data mining: why and how. *Phys. Reps.*, **635**, 1-44.

[7] Newman, M. E., Barabási, A. L., & Watts, D. J. *The structure and dynamics of networks* (Princeton university press, 2006).

[8] Dorogovtsev, S. N., & Mendes, J. F. *Evolution of networks: From biological nets to the Internet and WWW* (OUP Oxford, 2013).

[9] Chung, F. R., & Graham, F. C. *Spectral graph theory* (American Mathematical Soc., No 92, 1997).

[10] Dorogovtsev, S. N., Goltsev, A. V., Mendes, J. F., & Samukhin, A. N. (2003). Spectra of complex networks. *Phys. Rev. E*, **68**(4), 046109.

[11] Dorogovtsev, S. N., Goltsev, A. V., Mendes, J. F. F., & Samukhin, A. N. (2004). Random networks: eigenvalue spectra. *Physica A*, **338**(1-2), 76-83.

[12] Kim, D. H., & Motter, A. E. (2007). Ensemble averageability in network spectra. *Phys. Rev. Lett.*, **98**(24), 248701.

[13] Estrada, E., & Rodriguez-Velazquez, J. A. (2005). Subgraph centrality in complex networks. *Phys. Rev. E*, **71**(5), 056103.

[14] Pauls, S. D., & Remondini, D. (2012). Measures of centrality based on the spectrum of the Laplacian. *Phys. Rev. E*, **85**(6), 066127.

[15] Martin, T., Zhang, X., & Newman, M. E. (2014). Localization and centrality in networks. *Phys. Rev. E*, **90**(5), 052808.

[16] Van Mieghem, P., Ge, X., Schumm, P., Trajanovski, S., & Wang, H. (2010). Spectral graph analysis of modularity and assortativity. *Phys. Rev. E*, **82**(5), 056113.

[17] Nadakuditi, R. R., & Newman, M. E. (2012). Graph spectra and the detectability of community structure in networks. *Phys. Rev. Lett.*, **108**(18), 188701.

[18] Peixoto, T. P. (2013). Eigenvalue spectra of modular networks. *Phys. Rev. Lett.*, **111**(9), 098701.

[19] Denton, P. B., Parke, S. J., Tao, T., & Zhang, X. (2020). Eigenvectors from eigenvalues: a survey of a basic identity in linear algebra. arXiv:1908.03795v3.

[20] Denton, P. B., Parke, S. J., & Zhang, X. (2020). Neutrino oscillations in matter via eigenvalues. *Phys. Rev. D*, **101**(9), 093001.

[21] Klein, D. J., & Randić, M. (1993). Resistance distance. *Journal of Mathematical Chemistry*, **12**(1), 81-95.

[22] Chen, H., & Zhang, F. (2007). Resistance distance and the normalized Laplacian spectrum. *Discrete Applied Mathematics*, **155**(5), 654-661.

[23] Zhang, H., & Yang, Y. (2007). Resistance distance and Kirchhoff index in circulant graphs. *Int. J. Quantum Chem.*, **107**(2), 330-339.

[24] Rubido, N. (2016). Complex Networks. In *Energy Transmission and Synchronization in Complex Networks* (pp. 13-43). Springer, Cham.

[25] Asad, J. H., Sakaji, A., Hijjawi, R. S., & Khalifeh, J. M. (2006). On the resistance of an infinite square network of identical resistors–Theoretical and experimental comparison. *The European Physical Journal B-Condensed Matter and Complex Systems*, **52**(3), 365-370.

[26] Owaidat, M. Q., Asad, J. H., & Khalifeh, J. M. (2014). Resistance calculation of the decorated centered cubic networks: Applications of the Green's function. *Modern Physics Letters B*, **28**(32), 1450252.

[27] Rubido, N., Grebogi, C., & Baptista, M. S. (2017). Interpreting physical flows in networks as a communication system. In *Indian Academy of Sciences Conference Series*.

[28] Girvan, M., & Newman, M. E. J. (2002). Community structure in social and biological networks. *Proc. Natl. Acad. Sci.*, **99**(12), 7821-7826.

[29] Rubido, N., Grebogi, C., & Baptista, M. S. (2013). Structure and function in flow networks. EPL (*Europhysics Letters*), **101**(6), 68001.

[30] Zhang, T., & Bu, C. (2019). Detecting community structure in complex networks via resistance distance. *Physica A*, **526**, 120782.

[31] López, E., Buldyrev, S. V., Havlin, S., & Stanley, H. E. (2005). Anomalous transport in scale-free networks. *Phys. Rev. Lett.*, **94**(24), 248701.

[32] Wang, W. X., & Lai, Y. C. (2009). Abnormal cascading on complex networks. *Phys. Rev. E*, **80**(3), 036109.

[33] Katifori, E., Szöllösi, G. J., & Magnasco, M. O. (2010). Damage and fluctuations induce loops in optimal transport networks. *Phys. Rev. Lett.*, **104**(4), 048704.

[34] Rubido, N., Grebogi, C., & Baptista, M. S. (2014). Resiliently evolving supply-demand networks. *Phys. Rev. E*, **89**(1), 012801.

[35] Tyloo, M., Coletta, T., & Jacquod, P. (2018). Robustness of synchrony in complex networks and generalized Kirchhoff indices. *Phys. Rev. Lett.*, **120**(8), 084101.

[36] Tyloo, M., & Jacquod, P. (2019). Global robustness versus local vulnerabilities in complex synchronous networks. *Phys. Rev. E*, **100**(3), 032303.

[37] Kozma, B., Hastings, M. B., & Korniss, G. (2004). Roughness scaling for Edwards-Wilkinson relaxation in small-world networks. *Phys. Rev. Lett.*, **92**(10), 108701.

[38] Kozma, B., Hastings, M. B., & Korniss, G. (2005). Diffusion processes on power-law small-world networks. *Phys. Rev. Lett.*, **95**(1), 018701.

[39] Korniss, G. (2007). Synchronization in weighted uncorrelated complex networks in a noisy environment: Optimization and connections with transport efficiency. *Phys. Rev. E*, **75**(5), 051121.

[40] McRae, B. H., & Beier, P. (2007). Circuit theory predicts gene flow in plant and animal populations. *Proc. Natl. Acad. Sci.*, **104**(50), 19885-19890.

[41] Marrotte, R. R., & Bowman, J. (2017). The relationship

between least-cost and resistance distance. *PloS ONE*, **12**(3): e0174212.

[42] Thiele, J., Buchholz, S., & Schirmel, J. (2018). Using resistance distance from circuit theory to model dispersal through habitat corridors. *J. Plant Ecol.*, **11**(3), 385-393.

[43] Chang, K. C., Pearson, K., & Zhang, T. (2008). Perron-Frobenius theorem for nonnegative tensors. *Communications in Mathematical Sciences*, **6**(2), 507-520.

[44] Papendieck, B., & Recht, P. (2000). On maximal entries in the principal eigenvector of graphs. *Linear Algebra and its Applications*, **310**(1-3), 129-138.

[45] Bonacich, P. (2007). Some unique properties of eigenvector centrality. *Social Networks*, **29**(4), 555-564.

[46] Sharkey, K. J. (2019). Localization of eigenvector centrality in networks with a cut vertex. *Phys. Rev. E*, **99**(1), 012315.

[47] Lohmann, G., et al. (2010). Eigenvector centrality mapping for analyzing connectivity patterns in fMRI data of the human brain. *PloS ONE*, **5**(4): e10232.

[48] Martínez, J. H., Buldú, J. M., Papo, D., Fallani, F. D. V., & Chavez, M. (2018). Role of inter-hemispheric connections in functional brain networks. *Sci. Rep.*, **8**(1), 1-10.

[49] Binnewijzend, M. A., et al. (2014). Brain network alterations in Alzheimer's disease measured by eigenvector centrality in fMRI are related to cognition and CSF biomarkers. *Hum. Brain Map.*, **35**(5), 2383-2393.

[50] Martínez, J. H., Ariza, P., Zanin, M., Papo, D., Maestú, F., Pastor, J. M., ... & Buldú, J. M. (2015). Anomalous consistency in mild cognitive impairment: a complex networks approach. *Chaos, Solitons & Fractals*, **70**, 144-155.

[51] van Duinkerken, E., et al. (2017). Altered eigenvector centrality is related to local resting-state network functional connectivity in patients with longstanding type 1 diabetes mellitus. *Hum. Brain Map.*, **38**(7), 3623-3636.

[52] Luo, X., et al. (2017). Intrinsic functional connectivity alterations in cognitively intact elderly APOE ϵ4 carriers measured by eigenvector centrality mapping are related to cognition and CSF biomarkers: a preliminary study. *Brain Imaging and Behavior*, **11**(5), 1290-1301.

[53] Newman, M. E. J. (2006). Finding community structure in networks using the eigenvectors of matrices. *Phys. Rev. E*, **74**, 036104.

[54] Negre, C. F., et al. (2018). Eigenvector centrality for characterization of protein allosteric pathways. *Proc. Natl. Acad. Sci.*, **115**(52), E12201-E12208.

[55] Welch, P. M., & Welch, C. F. (2017). Eigenvector centrality is a metric of elastomer modulus, heterogeneity, and damage. *Sci. Reps.*, **7**(1), 1-8.

[56] Press, W. H., Teukolsky, S. A., Flannery, B. P., & Vetterling, W. T. *Fortran numerical recipes: the art of scientific computing* (Cambridge university press, Vol 1, 1992).

[57] Rubinov, M., Sporns, O. (2010). Complex network measures of brain connectivity: Uses and interpretations. *NeuroImage* **52**, 1059-69.

[58] Barabási, A. L., & Albert, R. (1999). Emergence of scaling in random networks. *Science*, **286**(5439), 509-512.

[59] Erdös, P., & Rényi, A. (1960). On the evolution of random graphs. *Publ. Math. Inst. Hung. Acad. Sci.*, **5**(1), 17-60.

[60] Watts, D. J., & Strogatz, S. H. (1998). Collective dynamics of "small-world" networks. *Nature*, **393**(6684), 440.

[61] Jacobi, C. G. J. (1834). De binis quibuslibet functionibus homogeneis secundi ordinis per substitutiones lineares in alias binas tranformandis, quae solis quadratis variabilium constant; una cum variis theorematis de tranformatione etdeterminatione integralium multiplicium. *Journal für die reine und Angewandte Mathematik*, **1834**(12), 1-69.

[62] Mäki-Marttunen, T., Aćimović, J., Ruohonen, K., Linne, M. L. (2013). Structure-dynamics relationships in bursting neuronal networks revealed using a prediction framework. *PLoS One* **8**:e69373.